INSTITUTE OF PHYSICS PUBLISHING NANOTECHNOLOGY
Nanotechnology **16** (2005) 1536–1541 doi:10.1088/0957-4484/16/9/022

Atomic nanolithography patterning of submicron features: writing an organic self-assembled monolayer with cold, bright Cs atom beams

C O'Dwyer[1,3], G Gay[1], B Viaris de Lesegno[1,4], J Weiner[1], A Camposeo[2], F Tantussi[2], F Fuso[2], M Allegrini[2] and E Arimondo[2]

[1] Institut de Recherche sur les Systèmes Atomiques et Moléculaires Complexes, Laboratoire de Collisions, Agrégats et Réactivité, Université Paul Sabatier, 118 route de Narbonne, 31062 Toulouse Cedex 4, France
[2] Dipartimento di Fisica Enrico Fermi, Instituto Nazionale per la Fisica della Materia, Università di Pisa, Via Buonarroti 2, I-56127 Pisa, Italy

Received 14 March 2005, in final form 26 May 2005
Published 29 June 2005
Online at stacks.iop.org/Nano/16/1536

Abstract
Cs atom beams, transversely collimated and cooled, passing through *material* masks in the form of arrays of reactive-ion-etched hollow Si pyramidal tips and *optical* masks formed by intense standing light waves, write submicron features on self-assembled monolayers (SAMs). Features with widths as narrow as 43 ± 6 nm and spatial resolution limited only by the grain boundaries of the substrate have been realized in SAMs of alkanethiols. The material masks write two-dimensional arrays of submicron holes; the optical masks result in parallel lines spaced by half the optical wavelength. Both types of feature are written to the substrate by exposure of the masked SAM to the Cs flux and a subsequent wet chemical etch. For the arrays of pyramidal tips, acting as passive shadow masks, the resolution and size of the resultant feature depends on the distance of the mask array from the SAM, an effect caused by the residual divergence of the Cs atom beam. The standing wave optical mask acts as an array of microlenses focusing the atom flux onto the substrate. Atom 'pencils' writing on SAMs have the potential to create arbitrary submicron figures in massively parallel arrays. The smallest features and highest resolutions were realized with SAMs grown on smooth, sputtered gold substrates.

The growth mechanism, application and physico-chemical properties of self-assembled monolayers (SAMs) of alkanethiol molecules on single-crystal Au surfaces have been studied by numerous groups [1, 2]. These monolayers self-assemble spontaneously on solid surfaces by cleavage of the S–H bond and subsequent chemisorption to the surface through a covalent Au–S bond. They provide a well defined, stable 'paper' on which nanoscale atom beams can write.

[3] Present address: Photonic Nanostructures Group, Tyndall National Institute, Cork, Republic of Ireland.
[4] Present address: Laboratoire Aimé Cotton, Campus d'Orsay, 91405 Orsay, France.

Over the last ten years, considerable research efforts have been devoted to developing processes for nanoscale feature definition below the optical diffraction limit of conventional lithography. The pioneering work of Timp *et al* [3, 4] and McClelland *et al* [5] used a standing optical wave to directly write a focused flux of neutral atoms onto a surface. Although the transverse velocity components of the atomic beams are optically cooled to millikelvin temperatures, the *longitudinal* velocity distribution is left uncooled and defined by the temperature of the atomic source oven. Since the de Broglie wavelength is of subnanometre order at conventional atomic beam temperatures, the deposited structure resolution is

not limited by matter–wave diffraction. McClelland deposited lines of Cr as narrow as 38 nm, spaced by 213 nm. These early studies stimulated several variants in the field of direct-write neutral atom nanolithography using optical masks and material masks [6].

An alternative to direct deposit, writing 'resists' on substrates in neutral atom nanolithography provides both high sensitivity and high resolution [7, 8]. The resists that show the best response to neutral atom lithography are those of self-assembled monolayers (SAMs) of organic molecules. Berggren and co-workers [9] have demonstrated the modification of the chemical properties of a thin film made from a self-assembled monolayer (SAM) of organic molecules on a surface. They used a beam of metastable argon atoms patterned by a material mask. Lithography at nanometre scales (<100 nm) requires resists thin enough and smooth enough that they yield features with reasonable aspect ratios between width and depth. Among the many SAM systems that have been investigated, those made by adsorbing alkanethiols on single-crystal gold surfaces have been most frequently studied because of their ease of preparation and excellent stability [10]. SAMs have particular advantages, compared to polymeric resists, for the fabrication of nanometre scale features. The molecular diameter of the species in the SAM is small (<1 nm) and the corresponding films sufficiently thin that they minimize scattering of incident particles or atoms within the film [9, 11]. To generate useful contrast between exposed and unexposed regions, a sufficient dose of atoms must be provided, but it must not over-expose to outlying regions. Furthermore, the structure formation is strongly affected by migration, agglomeration and local interaction of the atoms deposited on the surface. We have recently clarified the explicit behaviour of such properties [12], and optimized [13] the details of the atom–surface interaction that plays a crucial role in resist-write atomic nanolithography experiments.

The modification of the SAM on exposure, which is believed to stem from the Cs attack on the Au–S bond, allows replication of a lithographic material mask down to submicron dimensions. Such spatial resolution is possible due to the high density molecular coverage (4×10^{14} cm^{-2}) which corresponds to a small minimum molecular unit area of 4 nm^2. Recently, the feature sizes of patterns written into SAMs through techniques such as scanning near field photolithography (SNP) [14, 15], dip-pen nanolithography [16] and micro-contact printing [17, 18] have been shown to be limited by the morphology of the granular metal surface. We have recently reported [12] that a resolution limit of ∼20 nm is found when 1-nonanethiol SAMs are adsorbed on sputtered Au substrates. The results indicated that the quality of the Au surface is paramount in realizing a low defect density molecular SAM.

In this paper, we report the writing of submicron features patterned onto a self-assembled monolayer of alkanethiol on a Au substrate, using cold neutral Cs atom beams. Features were written to the SAM employing both material and optical masks. The material masks consisted of arrays of pyramidal tips etched from standard Si wafers. With these masks 230 nm diameter holes regularly spaced by 25 μm were written into the SAM. The sharpness or spatial gradient of the holes was limited only by the uniformity of the SAM surface. Employing optical standing wave masks, we were able to expose lines with a period spacing of 426 nm and an average width of 43 ± 6 nm. By translating the SAM surface transverse to the atom flux, these masking tools can be used to write massively parallel figures of arbitrary and periodic form.

Samples were prepared on sputtered Au films which contained predominantly {111} oriented Au grains and an associated roughness of 1.8 ± 0.4 nm. Details of the Au substrates can be found in [12, 13]. A self-assembled monolayer of 1-nonanethiol $CH_3(CH_3)_8SH$ of thickness ∼1 nm was grown on the surface. Etching of exposed samples was carried out using an aqueous oxidizing etching solution. Atomic force microscopy (AFM) and scanning tunnelling microscopy (STM) characterization was performed with a Veeco Multiprobe Nanoscope IV and a Pacific Nanotechnologies Nano-R. Further details on sample preparation and surface morphological analysis can be found elsewhere [12, 13].

By employing the optimizations reported previously [13] for Cs beam exposure of the alkanethiol layer and the etching process, we have been successful in realizing submicron features using both material masks and optical standing wave masks. The experiments on material masks were carried out in Toulouse, the experiments on optical masks in Pisa. The following are brief descriptions of the set-ups used in these experiments.

Figure 1(a) shows a schematic diagram of the Toulouse Cs beam used to expose the SAM through the material masks. A thermal oven source heats a Cs metal reservoir to 373 K; the Cs atomic beam effuses through an output nozzle, a long narrow tube 36 mm in length, 1.6 mm in diameter. Optical molasses [19] cools the transverse velocity components of the beam, resulting in a 'bright' [20] Cs atom beam, highly collimated to a divergence <1 mrad along the z direction. The beam has an average forward velocity of 150 m s^{-1}, a forward flux density of 10^{12} atoms cm^{-2} s^{-1} and a residual divergence of <1 mrad.

The atom lithography apparatus developed in Pisa (figure 1(b)) uses a beam of cold Cs atoms, produced out of a pyramidal magneto-optical trap (MOT) [21]. In this arrangement both the longitudinal and transverse velocity components are cooled. This source of cold Cs atoms is able to produce a continuous flux of cold Cs when a suitably tuned and arranged laser beam is directed into the pyramid, so that the configuration of a standard six-beam MOT is reproduced. The atomic beam extracted from the pyramidal MOT source has a flux of 4×10^9 atoms s^{-1}, a divergence of 26 mrad, a longitudinal velocity of 10 m s^{-1}, and a longitudinal velocity spread of 1.5 m s^{-1}. The divergence of the atomic beam is reduced by a further collimation stage [22] based on a standard transverse optical molasses cooling which results in a beam divergence of ∼4 mrad. The properties of the two cold Cs beams are summarized in table 1.

The Toulouse experiment employed pyramidal tip masks and Pisa used the optical standing wave. A detailed description of the fabrication process for the pyramidal tip array masks can be found elsewhere in [13, 23, 24]. We show in figure 2 a scanning electron microscope (SEM) image of a typical mask. Figure 3 shows AFM images of SAMs exposed for 15 min through the pyramidal masks. The apertures used have a diameter of 300 nm. The exposed SAM was

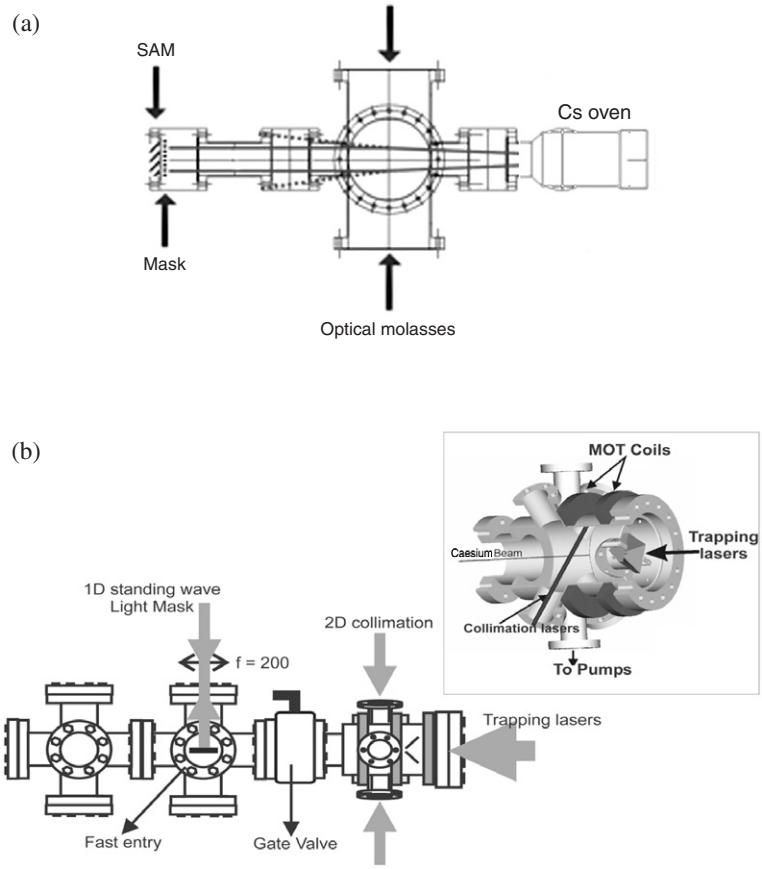

Figure 1. Schematic diagram of the two Cs atomic beams. (a) Toulouse beam: the source is a thermal oven heated about 75 K above ambient temperature. An effusive beam issuing from the nozzle is collimated by transverse optical molasses that cools the transverse velocity components. The cross section of the beam is $\simeq$3 mm, and the residual divergence is $\sim$1 mrad. The Cs flux passes through an array of pyramidal-tip masks (figure 2) and deposits on the SAM substrate. (b) Pisa beam: a cloud of cold atoms is formed in a pyramidal magneto-optical trap (shown in inset) and extracted into the slow Cs beam. The pyramid is formed by two mirrors and two reflecting prisms, arranged to obtain a square pyramid, with a 38 $\times$ 38 mm^2 base. The pyramid set-up is enclosed in a 100 mm diameter cylindrical vacuum chamber.

Table 1. Summary of the properties of the cold caesium beams at Pisa and Toulouse.

Atom beam property	Pisa	Toulouse
Flux (atoms s^{-1})	4×10^9	3×10^{11}
Flux density (atoms s^{-1} cm^{-2})	3×10^{10}	10^{12}
Longitudinal velocity (m s^{-1})	10	150
Longitudinal velocity spread (m s^{-1})	1.5	150
Beam area (mm^2)	20	10
Divergence (mrad)	4	1

subsequently developed in the water-based etchant according to the procedures outlined in [13]. In figure 3(a), the aperture was placed 363 μm above the SAM surface. The resultant feature exhibits an irregular periphery and has a maximum diameter of 512 nm. Furthermore, line scans through the etched feature show the sidewall fractional depth gradient (ratio of normalized height to width in nanometres) to be 0.47/20 nm^{-1}. The feature width is $\sim$200 nm greater than the aperture diameter and is caused by the divergence of the transmitted Cs atomic beam. A residual divergence of $\sim$1 mrad exists within the Cs atomic beam after the transverse optical molasses collimation stage. Figure 3(b) shows the resulting etched feature when the 300 nm aperture was placed 16 μm above the SAM surface and exposed for 15 min. The diameter of the feature is significantly reduced from that of figure 3(a), with a corresponding fractional depth gradient of 0.8/20 nm^{-1}. This excellent feature resolution is observed in the roundness of the etched feature, indicating a uniform Cs flux distribution emanating from the circular aperture. Pyramidal tips with smaller diameters were also employed, and figure 4 shows an AFM image and associated line scan of an etched feature after being exposed through a pyramidal mask with an aperture diameter of 140 nm, placed 16 μm above the SAM.

For the Pisa experiments SAM samples were exposed using optical masks. The basic principle of the light mask operation relies on the occurrence of a conservative force, known as the optical gradient dipole force $\vec{F}_{\rm dip}$ [25], experienced by neutral atoms as they traverse the periodic intensity gradients of a standing-wave electromagnetic field:

$$\vec{F}_{\rm dip} = -\frac{\hbar\Gamma^2}{8\Delta I_{\rm s}}\vec{\nabla} I(\vec{r}), \tag{1}$$

where Γ is the natural line width of the atomic resonance, Δ is the frequency detuning of the laser from the atomic resonance, I is the electromagnetic field intensity, and $I_{\rm s}$ is

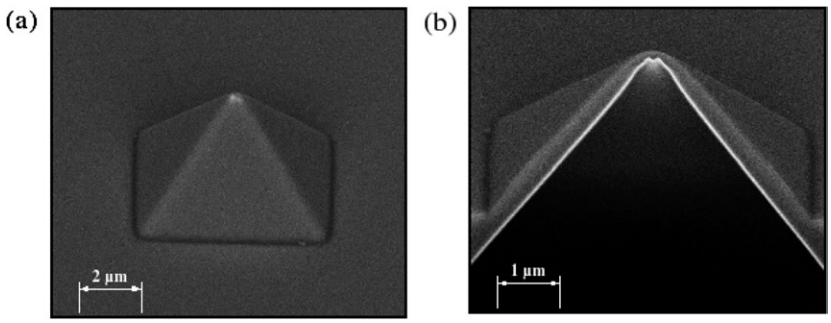

Figure 2. (a) A secondary electron microscopy (SEM) image of the pyramidal tips. Panel (a) shows one of the pyramidal structures with a 300 nm hole in the apex of the tip. The base of the pyramid, as shown after the wet-etch process, is 3.5 μm on a side. The overall base of the pyramidal structure is 22 μm on a side. Panel (b) shows a focused ion beam (FIB) milled cross-section of the pyramidal tip aperture.

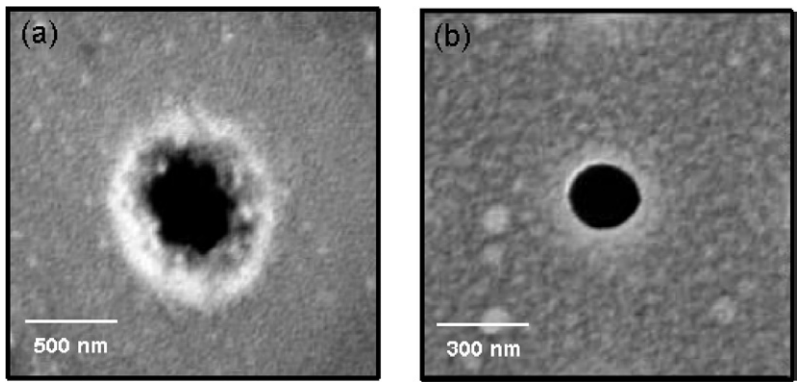

Figure 3. AFM image of the etched SAM substrate exposed for 15 min to the Cs atom flux through the pyramidal tip mask. The pyramidal tip is pointed toward the atomic beam source. The mask aperture is (a) 363 μm and (b) 16 μm above the SAM surface; the aperture diameter is 300 nm. Grey scale indicates relative height, and the white ring in (a) represents the depth gradient from the top of the SAM to the fully etched Si substrate (black).

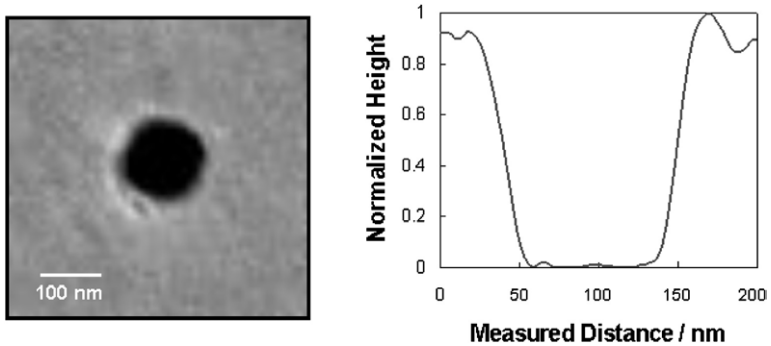

Figure 4. AFM image (left) and measured profile (right) of the etched SAM substrate exposed for 15 min to the Cs atom flux through the pyramidal tip mask. The pyramidal tip is pointed toward the atomic beam source. The mask aperture is 16 μm above the SAM surface; the aperture diameter is 140 nm. The depth is ∼35 nm. The fractional depth gradient is measured to be $0.8/20\ \mathrm{nm}^{-1}$.

the saturation intensity associated with the atomic resonance. For Cs, $\Gamma = 2\pi \times 5.22$ MHz and $I_s = 1.1$ mW cm^{-2}.

A direct consequence of equation (1) is the possibility of focusing atoms with a one-dimensional standing wave, the simplest light mask that can be realized. By retroreflecting a laser beam propagating along an axis transverse to the atom beam, the light intensity in the resulting standing wave has a spatially dependent amplitude proportional to $\sin^2(kx)$, where $\mathbf{k} = (2\pi/\lambda)\hat{\mathbf{x}}$ is the wavevector of propagation. If the frequency of the light is tuned slightly to the blue of the Cs resonance line, the atom flux traversing the standing wave will be pushed towards the standing wave nodes. The light field behaves as an array of cylindrical lenses for atoms, spaced by $\lambda/2$. The parameters of the standing wave are chosen to produce channelling of the atoms in the standing wave. Numerical trajectory simulations indicate that this channelling regime produces the smallest structures, given the residual divergence of the Pisa atom beam. Experimentally,

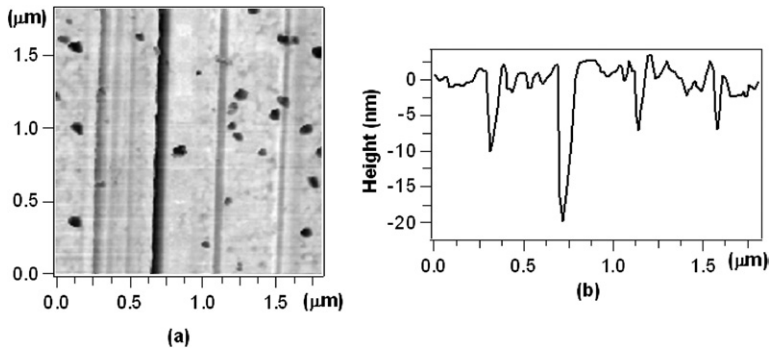

Figure 5. (a) AFM image of the SAM surface after exposure to a Cs atom flux passing through a standing wave optical mask. Black dots are etch pits arising from pinholes in the SAM. (b) Trench line profile from panel (a) showing the periodic patterning of lines at $\lambda = 426$ nm.

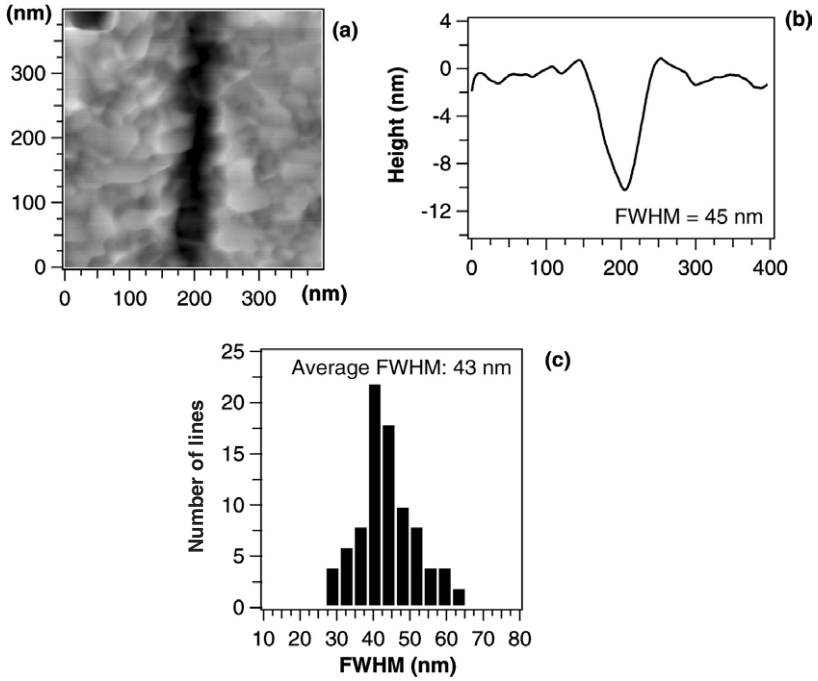

Figure 6. (a) AFM image of a single line obtained with a sputtered gold substrate, 30 nm thick. (b) Profile analysis of a single line, summed over 1 μm line length. (c) Histogram of the line widths. The average line width is 43 nm.

the optical standing wave is positioned immediately above the SAM surface, and the laser is tuned 1 GHz to the blue of the Cs D2 resonance line. To enhance the light intensity in the interaction region, we tightly focus the laser beam to a waist of 100 μm parallel to the atom beam axis and adjust the SAM substrate such that it is positioned on the maximum of the transverse Gaussian profile of the standing wave. Due to the slow longitudinal velocity of the Pisa atom beam, we achieve a relatively long interaction time ($\sim$10 μs).

Due to the beam segregation, which guides atoms into well defined spatial regions, there is a local flux enhancement of a factor of five according to the numerical simulations. Thus, minimum exposure time for the nanopatterned samples is expected to be reduced by a factor of five compared to nonchannelling material masks. We chose an exposure time of 2 h, corresponding to an estimated dose of 2 Cs atoms per nonanethiol molecule [13]. Subsequent wet-etching for the optimized time at room temperature ensured writing of the features into the substrate.

In order to assess the presence of a pattern with the expected periodicity, we first characterized the samples by diffraction measurements. The periodic pattern transferred to the gold substrate acts as a diffraction grating for visible light. The grating period d can be easily derived by varying the illumination wavelength and measuring the corresponding diffraction angles. By using the grating diffraction law,

$$\cos\vartheta_{\mathrm{i}} + \cos\vartheta_{\mathrm{d}} = \frac{m\lambda}{d} \tag{2}$$

$m = 0, \pm, \pm 2, \ldots$ being an integer number, λ the wavelength of the radiation, ϑ_{i} and ϑ_{d} the incident and diffracted angles respectively, the grating period d can be derived. Samples that show diffraction at the expected angles for different wavelengths were imaged by AFM. An example is shown in figure 5. The AFM analysis of this sample has shown the

presence of regions where parallel lines spaced by 426 nm are present. The inhomogeneity of the measured etch depth (figure 5(b)) arises from nonuniform etching of the gold layer. This nonuniformity in etch depth or etch rate was not observed in the Toulouse experiments, and we speculate that the use of a slow Cs flux may result in a reduced Cs-SAM 'damage' rate.

In figure 6(a), we report an AFM image of a single trench. The edges of the lines follow the grain distribution of the gold film, suggesting that the ultimate resolution of the technique is limited by the grain size of the gold film. Figure 6(b) shows the line profile of a single trench averaged over 1 μm trench length. The resulting line width (FWHM) is 45 nm. We have analysed the width distribution over the imaged trenches in all the acquired scans. The resulting histogram is shown in figure 6(c). The line width ranges through 30–65 nm, with an average value of 43 nm.

It is observed that the morphology of the grains in the gold layer has a strong effect on written feature sizes with the feature edges delineated by the grain boundaries. Similar observations have also been noted for scanning near-field photolithography and for dip-pen nanolithography, implying a non-process-dependent resolution limit to alkanethiol/Au based subwavelength lithographic techniques [14, 15]. However, we have recently shown that even on a perfect single-crystal Au surface the resolution is limited to $\sim$20 nm due to inhomogeneities in the self-assembly mechanism of methyl-terminated alkanethiols, specifically on {111}-oriented surfaces [12].

Thus, submicron sized lines and holes have successfully been written to alkanethiol monolayers adsorbed on Au surfaces with excellent edge resolution by Cs-beam-mediated atomic nanolithography. Features have been written using novel material masks as well as optical standing wave masks. For the pyramidal tip masks, studies of write speed versus clogging rate are in progress, while for the optical masks the role played by the atom beam longitudinal velocity in the SAM damage rate must be investigated. These technologies may find application in atoms-on-demand deposition, precision doping, and nanoscale lithography using mask arrays to write many arbitrary figures in parallel.

Acknowledgments

This work was supported in part by the European Community's IST Programme under contract IST-2001-32264, Région Midi-Pyrénées under contract SFC/CR 02/22, under the ACI Nanosciences Nanotechnologies Programme of the Ministere de l'Education Nationale, de l'Enseignement Supèrieur et de Recherche, and under the FIRB Project RBAU01S22E of the Ministero Italiano dell'Università e della Ricerca, MIUR. One of the authors (CO'D) also acknowledges the financial support provided through the European Community's Human Potential Programme under contract HPRN-CT-2002-00304. We are grateful to Martin Mueller for the substrate preparation and to R Solaro and M Alderighi for use of and assistance with the AFM system, respectively.

References

[1] Schreiber F 2000 *Prog. Surf. Sci.* **65** 151
[2] Ulman A 1996 *Chem. Rev.* **96** 1533
[3] Timp G L, Behringer R L, Tennant D M, Cunningham J E, Prentiss M and Berggren K K 1992 *Phys. Rev. Lett.* **69** 1636
[4] Prentiss M, Timp G, Bigelow N, Behringer R E and Cunningham J E 1992 *Appl. Phys. Lett.* **60** 1027
[5] McClelland J J, Scholten R E, Palm E C and Celotta R J 1997 *Science* **262** 877
[6] Meschede D and Metcalf H 2003 *J. Phys. D: Appl. Phys.* **36** R17 and references cited therein
[7] Younkin R, Berggren K K, Johnson K S, Prentiss M, Ralph D C and Whitesides G M 1997 *Appl. Phys. Lett.* **71** 1261
[8] Berggren K K, Younkin R, Cheung E, Prentiss M, Black A K J, Whitesides G M, Ralph D C, Black C T and Tinkham M 1997 *Adv. Mater.* **9** 52
[9] Berggren K K, Bard A, Wilbur J L, Gillaspy J D, Helg A G, McClelland J J, Rolston S L, Phillips W D, Prentiss M and Whitesides G M 1995 *Science* **269** 1255
[10] Walczak M M, Alves C A, Lamp B D and Porter M D 1995 *J. Electroanal. Chem.* **396** 103
[11] Tiberio R C, Craighead H G, Lercel M, Lau T, Sheen C W and Allara D L 1993 *Appl. Phys. Lett.* **62** 476
[12] O'Dwyer C, Gay G, Viaris de Lesegno B and Weiner J 2004 *Langmuir* **20** 8172
[13] O'Dwyer C, Gay G, Viaris de Lesegno B, Weiner J, Ludolph K, Albert D and Oesterschulze E 2005 *J. Appl. Phys.* **97** 114309
[14] Sun S and Leggett G J 2002 *Nano Lett.* **2** 1223
[15] Sun S, Chong K S L and Leggett G J 2002 *J. Am. Chem. Soc.* **124** 2414
[16] Xia Y and Whitesides G M 1998 *Annu. Rev. Mater. Sci.* **28** 153
[17] Xia Y, Zhao X M and Whitesides G M 1996 *Micro. Eng.* **32** 255
[18] Wilbur J L, Kumar A, Biebuyck H A, Kim E and Whitesides G M 1996 *Nanotechnology* **7** 452
[19] An introduction to the physics of optical cooling and trapping can be found in two special issues of the Journal of the Optical Society of America B. These are:
Meystre P and Stenholm S 1985 *J. Opt. Soc. Am.* B **2** (11)
Chu S and Wieman C 1989 *J. Opt. Soc. Am.* B **6** (11)
[20] DeGraffenreid W, Liu Y-M, Ramirez-Serrano J and Weiner J 2000 *Rev. Sci. Instrum.* **70** 3668
[21] Camposeo A, Piombini A, Cervelli F, Tantussi F, Fuso F and Arimondo E 2001 *Opt. Commun.* **200** 231
[22] Camposeo A, Cervelli F, Piombini A, Tantussi F, Fuso F, Allegrini M and Arimondo E 2003 *Mater. Sci. Eng.* C **23** 217
[23] Vollkopf A, Rudow O and Oesterschulze E 2001 *J. Electrochem. Soc.* **148** G587
[24] Georgiev G, Müller-Wiegand M, Georgieva A, Ludolph K and Oesterschulze E 2003 *J. Vac. Sci. Technol.* B **21** 1361
[25] Metcalf H J and van der Straten P 1999 *Laser Cooling and Trapping* (New York: Springer) p 151